CONTROLLED DRUG DELIVERY IN CANCER IMMUNOTHERAPY: STABILITY, OPTIMIZATION, AND MONTE CARLO ANALYSIS

ANDREA MINELLI *, FRANCESCO TOPPUTO†, AND FRANCO BERNELLI-ZAZZERA‡

Abstract. A discussion on controlled drug delivery in cancer immunotherapy is presented in this paper. A fifth-order model is adopted to describe the dynamics of the tumor–immune interaction. Natural equilibrium points of this system are sought, and their stability is analyzed. An optimal control problem is stated and solved numerically. Both continuous and discrete controls are treated, and their implications on the therapy protocol are discussed. The robustness of the optimal therapies is assessed a posteriori with a Monte Carlo analysis. This shows that the control policy is effective even with uncertain patient's initial conditions.

Key words. cancer immunotherapy, optimal control, monte carlo analysis.

AMS subject classifications. 49M37, 92B05.

1. Introduction. Cancer is one of the five leading causes of death in all age groups among both males and females. Cancer is the leading cause of death among men and women under age 85 years [1]. Among the different kind of neoplasia, the number of melanoma cases worldwide is increasing faster than any other cancer and remains one of the most treatment-refractory cancers. Patients with metastatic melanoma have a life expectancy of less than five years in 95% of the cases [2]. Despite decades of clinical trials testing chemotherapy, a standard first line treatment has not yet been established. The disappointing results with single and multiple agent chemotherapy led to the evaluation of alternative treatments.

The relationship between melanoma and the immune system has been recognized for decades [3]. Case reports of spontaneous tumor regression in patients with metastatic melanoma have suggested that immunotherapy can influence the regression of the tumor growth [4]. Immunotherapy can be viewed as an external help that stimulates and increases the performances of the immune system [5, 6]. The purpose of the immune system is to protect against disease by identifying and killing pathogens and tumor cells. This is done with innate immune response and adaptive immune response [4, 7]. Innate immune response is rapid but less specific than the adaptive response; it includes physicochemical barriers (e.g., skin and mucosa), blood proteins, and phagocyte cells. Adaptive immunity is instead more specific and consists in the ability to recognize and remember specific pathogens, and to mount stronger attacks each time the pathogen is encountered.

Modeling and simulating the interactions between the immune system and the neoplasia is getting more and more interest. Rather than providing insights into experimental results, these models can be used as a valuable means to asses the impact of new therapies before clinical application. The tumor–immune interaction can be modeled with several mathematical means, such as ordinary or partial differential equations [7, 8], stochastic models [9], and agent-based models [10]. Among these,

*Applied Aerodynamics Department, Onera, 8 Rue des Vertugadins, 92160 Meudon, France (andrea.minelli@onera.fr).

†Dipartimento di Ingegneria Aerospaziale, Politecnico di Milano, Via La Masa 34, 20156, Milano, Italy (francesco.topputo@polimi.it)

‡Dipartimento di Ingegneria Aerospaziale, Politecnico di Milano, Via La Masa 34, 20156, Milano, Italy (franco.bernelli@polimi.it)

we use ordinary differential equations that model the evolution of the population concentration of the different cells as a continuous process. This is the mathematical framework suitable for applying the proposed optimal control methods.

One of the first attempts to model clinical treatment and immunotherapy has been done by Kirschner and Panetta [11]. In this study, a therapy based on injections of Interleukin-2 (IL-2) together with an adoptive cellular immunotherapy is considered. This model studies the dynamics of the tumor at different antigenicity levels. It consists of three differential equations describing the evolutions of tumor cells, immune-effector cells, and IL-2. No optimal control protocol is considered in [11]. This is done in [12] where the control policy is designed to maximize both the effector cells and IL-2, and to minimize the tumor cells. The same task has been done in [13] by introducing impulse-like administrations. In this latter case, both the timing and drug dosage are optimized. In [14], the global dynamics of the Kirschner and Panetta model is studied to determine the tumor clearance conditions. A mathematical model supporting the clinical use of Interleukin-21 (IL-21) is presented in [15]. This is a system of six differential equations with one input, IL-21, where model coefficients are found through a parameter estimation procedure. Modeling and controlling cancer dynamics is the subject of the work by Castiglione and Piccoli [16, 17]. Their model describes the tumor-immune interaction by means of a system of five differential equations; the control is represented by injection of dendritic cells. This model can be thought as an improvement to that by Kirschner and Panetta. In [17] continuous, discrete, and hybrid optimal control strategies are considered. A twelfth order system is used in [18] to model mammary carcinoma. Models combining chemo and immunotherapy are instead considered in [19, 20].

Previous works dealing with optimal control in cancer immunotherapy have approached the problem with the Pontryagin maximum principle [12, 13, 16, 17]; this is also called indirect method. In this framework, the Euler–Lagrange equations are derived, and the optimal solution is found by solving the associated two-point boundary value problem. Nevertheless, the lack of meaning of the Lagrange multipliers, together with the highly nonlinear dynamics characterizing the tumor-immune interaction, make it difficult to find a solution when the optimal control problem is stated in this way. For instance, in [16, 17] two control strategies have been introduced (continuous and discrete) but it has not been possible to solve the associated indirect optimal control problems. A third, hybrid problem is in fact formulated to circumvent these difficulties [17]. Moreover, all problems are stated in a fixed final time form.

In this work we elaborate on the model and on the two problems presented (and not solved) in [17]. The idea behind our study is to show that the continuos and discrete control cases can be treated and solved with a direct approach. (In doing so, we apply algorithms developed to solve problems in aerospace engineering [21]).

The paper is organized as follows. Firstly, the natural dynamics (i.e., with no control input) of the system are studied, and natural equilibrium points are searched globally. This is done analytically by exploiting the structure of the nonlinear vector field. The linear stability is analyzed, and the lack of stable, tumor-free equilibria is discussed. Secondly, the optimal control problem is formulated and solved using direct methods. In this paper, we use direct transcription and collocation for continuous control, and direct transcription and multiple shooting for discrete control. A genetic algorithm is implemented to deliver good first guess solutions to the latter. Optimal protocols are presented and discussed. In our approach, the final time is treated as an optimization parameter to find the optimal therapy duration. In the third part of

the paper the optimal control laws are used to run a Monte Carlo analysis. This step aims at assessing the robustness of optimal control laws when initial conditions are not known precisely, thus left free to vary. We show that even in these off-nominal cases the optimal protocol is able to reach a final state which is sufficiently close to the nominal minimum tumor state.

The goals of the paper are: 1. to perform a linear stability analysis of the Castiglione and Piccoli model [16, 17]; 2. to show that the continuous and discrete control problems can be solved with a direct transcription approach, and to solve both problems with variable therapy duration; 3. to assess the robustness of the continuous and discrete solutions when the initial patient conditions are affected by uncertainties.

The remainder of the paper follows. In Section 2 the dynamical model is briefly recalled. Equilibria and stability are studied in Section 3. In Section 4 the optimal control problem is formulated and approached with direct transcription algorithms. Both continuous and discrete solutions are presented in Section 5. The Monte Carlo analysis is carried out in Section 6, and final considerations are drawn in Section 7.

2. Tumor-Immune Dynamics. The tumor antigen is an antigenic substance produced in tumor cells that triggers an immune response in the host. The Tumor Associated Antigen (TAA) presentation occurs by means of dendritic cells. In autologous dendritic cell transfection therapy, the dendritic cells are extracted from the patient, loaded with a known TAA, and injected back into the patient. Their introduction ignites the response against the tumor cells. The tumor–immune interaction considered in this paper models the dynamics of the dendritic cell transfection. The model input is represented by dendritic cells. The fifth-order model is

$$\dot{H} = a_0 + b_0 DH(1 - H/f_0) - c_0 H, \quad \dot{C} = a_1 + b_1 I(M + D)C(1 - C/f_1) - c_1 C,$$

$$\dot{M} = b_2 M(1 - M/f_2) - d_2 MC, \quad \dot{D} = -d_3 DC + u, \quad \dot{I} = b_4 DH - e_4 IC - c_4 I. \tag{2.1}$$

System (2.1) describes the population dynamics of helper CD4 T-cell (H), cytotoxic CD8 T-cell (C), tumor cells (M), dendritic cells (D), and interleukin-2 (I). The fundamental time unit is one hour (see [17] for model assumptions). Table 2.1 reports the model coefficients and their values.

Coeff.	Description	Value	Unit
a_0	CD4 T birth rate	10^{-4}	$\mathrm{c\,h^{-1}mm^{-3}}$
b_0	CD4 T proliferation rate	10^{-1}	$\mathrm{c^{-1}h^{-1}mm^{-3}}$
c_0	CD4 T death rate	0.005	$\mathrm{h^{-1}}$
f_0	Carrying capacity of CD4 T	1	$\mathrm{c\,mm^{-3}}$
a_1	CD8 T birth rate	10^{-4}	$\mathrm{c\,h^{-1}mm^{-3}}$
b_1	CD8 T proliferation rate	10^{-2}	$\mathrm{c^{-1}h^{-1}mm^{-3}}$
c_1	CD8 T death rate	0.005	$\mathrm{h^{-1}}$
f_1	Carrying capacity of CD8 T	1	$\mathrm{c\,mm^{-3}}$
b_2	1/2 saturation const of tumor	0.02	$\mathrm{h^{-1}}$
d_2	killing by CD8 of tumor	0.1	$\mathrm{c^{-1}h^{-1}mm^{-3}}$
f_2	Carrying capacity of tumor	1	$\mathrm{c\,mm^{-3}}$
d_3	CD8 T killing of DC	0.1	$\mathrm{c^{-1}h^{-1}mm^{-3}}$
b_4	IL-2 production by CD4 T	10^{-2}	$\mathrm{c^{-1}h^{-1}mm^{-3}}$
c_4	IL-2 degradation rate	10^{-2}	$\mathrm{h^{-1}mm^{-3}}$
e_4	IL-2 uptake by CD8 T	10^{-7}	$\mathrm{c^{-1}h^{-1}mm^{-3}}$

TABLE 2.1

Coefficients of the model (taken from [17]); (c=cell, h=hour, mm=millimeter).

2.1. Comment to the Model. The first equation models the concentration of the tumor-specific CD4 cells (H). The terms a_0 and $-c_0H$ represent the rate of birth and natural death of cells, respectively. The term $b_0DH(1-H/f_0)$ is the proliferation of CD4 cells induced by dendritic cells. The saturation is taken into account through $1-H/f_0$: H increases when $H < f_0$ and decreases when $H > f_0$, where f_0 is the carrying capacity of CD4 cells. The second equation deals with tumor-specific CD8 cells (C). The terms a_1 and $-c_1C$ describe the rate of birth and natural death of cells, respectively. The term $b_1I(M+D)C(1-C/f_1)$ models the interaction of CD8 cells with IL-2, tumor, and dendritic cells. The saturation of CD8 cells is considered through $1-C/f_1$, being f_1 the upper bound. The dynamics of tumor cells (M) is described by the third equation. The term $b_2M(1-M/f_2)$ models proliferation and saturation of tumor cells (f_2 is the carrying capacity). The law of growth of tumor cells is of logistic type and is based on experimental data [22]. The term $-d_2MC$ that causes tumor regression is directly proportional to the concentration of CD8 cells. The fourth equation describes the concentration of dendritic cells (D). These cells act as an activator on CD8 cells (second equation). The term $-d_3DC$ models the destruction of dendritic cells when a certain number of CD8 cells is activated. The injection of dendritic cells, u, is the control variable. (It is assumed that dendritic cells specific for the tumor are prepared in vitro and then administered.) The last equation describes the dynamics of interleukin IL-2 (I). The term $-c_4I$ is the natural death rate, whereas $-e_4IC$ describes the decay of IL-2 after the immune system response is stimulated. Increase of IL-2 due to dendritic and CD4 cells is modeled through b_4DH. System (2.1) is scaled with the five states varying between 0 and 1, the latter being the scaled carrying capacity of cells per mm^3 [16]. Thus, in our analysis below, 0 means no cells, and 1 is the upper bound of all cells.

3. Stability of Equilibria. It is interesting to study the natural equilibrium points of system (2.1) when no treatment is considered (i.e., $u = 0$). This analysis is useful as possible stable equilibrium points with low (or no) tumor may be used as target of the optimal control policy. To this aim, we have to solve the nonlinear algebraic system

$$a_0 + b_0DH(1-H/f_0) - c_0H = 0, \tag{3.1}$$
$$a_1 + b_1I(M+D)C(1-C/f_1) - c_1C = 0, \tag{3.2}$$
$$b_2M(1-M/f_2) - d_2MC = 0, \tag{3.3}$$
$$-d_3DC = 0, \tag{3.4}$$
$$b_4DH - e_4IC - c_4I = 0, \tag{3.5}$$

with model coefficients given in Table 2.1. We notice that the trivial equilibrium (all states set to zero) is not possible as (3.1) and (3.2) would not be verified. System (3.1)–(3.5) is nonlinear and its solution would require a numerical method. However, the information in (3.4) can be used in a fruitful way. As $d_3 > 0$, (3.4) requires $DC = 0$. This can be achieved in three cases: i) $C = D = 0$; ii) $C = 0$, $D \neq 0$; iii) $C \neq 0$, $D = 0$. Cases i) and ii) have to be discarded as (3.2) is again not verified for $C = 0$ since $a_1 > 0$. In iii), condition $D = 0$ yields both $H = a_0/c_0$ from (3.1) and $I = 0$ from (3.5) (note that c_4, e_4 are both positive, therefore $I(e_4C + c_4) = 0$ in (3.5) has only solution $I = 0$ with $C \in [0, 1]$). The only equation left to solve is the tumor growth law

$$M\left[b_2\left(1-\frac{M}{f_2}\right) - d_2C\right] = 0 \tag{3.6}$$

with $C = a_1/c_1$, obtained by substituting $I = 0$ into (3.2). Equation (3.6) has the two solutions $M = 0$ and $M = f_2[1 - a_1 d_2/(b_2 c_1)]$. Summarizing, the dynamical system (2.1) has only two equilibrium points $P_1 = (H_1, C_1, M_1, D_1, I_1)$, $P_2 = (H_2, C_2, M_2, D_2, I_2)$ defined by

$$H_{1,2} = \frac{a_0}{c_0}, \quad C_{1,2} = \frac{a_1}{c_1}, \quad \begin{cases} M_1 = 0, \\ M_2 = f_2[1 - a_1 d_2/(b_2 c_1)], \end{cases} \quad D_{1,2} = 0, \quad I_{1,2} = 0.$$

With the model coefficients in Table 2.1, the coordinates of the equilibria are $P_1 = (0.02, 0.02, 0, 0, 0)$, $P_2 = (0.02, 0.02, 0.9, 0, 0)$.

The stability of P_1, P_2 can be inferred by the eigenvalues of the Jacobian [17]

$$J(P) = \begin{bmatrix} b_0 D(1 - 2H/f_0) - c_0, & 0, & 0, & b_0 H(1 - H/f_0), & 0 \\ 0, & b_1 I(M + D)(1 - 2C/f_1) - c_1, & b_1 IC(1 - C/f_1), & b_1 IC(1 - C/f_1), & b_1 C(M + D)(1 - C/f_1) \\ 0, & -d_2 M, & b_2(1 - 2M/f_2) - d_2 C, & 0, & 0 \\ 0, & -d_3 D, & 0, & -d_3 C, & 0 \\ b_4 D, & -e_4 I, & 0, & b_4 H, & -e_4 C - c_4 \end{bmatrix}. \tag{3.7}$$

For the first equilibrium point, the eigenvalues of $J(P_1)$ read

$$\begin{gathered} \lambda_1^{(1)} = -c_0, \quad \lambda_2^{(1)} = -c_1, \quad \lambda_3^{(1)} = -(a_1 d_2 - b_2 c_1)/c_1, \\ \lambda_4^{(1)} = -a_1 d_3/c_1, \quad \lambda_5^{(1)} = -(a_1 e_4 + c_1 c_4)/c_1, \end{gathered} \tag{3.8}$$

whereas the eigenvalues of $J(P_2)$ are

$$\begin{gathered} \lambda_1^{(2)} = -c_0, \quad \lambda_2^{(2)} = -c_1, \quad \lambda_3^{(2)} = (a_1 d_2 - b_2 c_1)/c_1, \\ \lambda_4^{(2)} = -a_1 d_3/c_1, \quad \lambda_5^{(2)} = -(a_1 e_4 + c_1 c_4)/c_1. \end{gathered} \tag{3.9}$$

As model coefficients are all positive, the eigenvalues are all negative except for $\lambda_3^{(1)}$ or $\lambda_3^{(2)}$ (note that $\lambda_3^{(1)} = -\lambda_3^{(2)}$, and $\lambda_i^{(1)} = \lambda_i^{(2)} < 0$, $i = 1, 2, 4, 5$). The stability of the two equilibria depends on the sign of $a_1 d_2 - b_2 c_1$. Thus, if $a_1 d_2 > b_2 c_1$ then and P_1 is stable and P_2 is unstable (case 1). On the contrary, if $a_1 d_2 < b_2 c_1$, P_1 is unstable and P_2 is stable (case 2). Biologically speaking, this means that if the ratio between birth and death rate of CD8 T-cell (a_1/c_1) is greater than the ratio between tumor growth and tumor killing (b_2/d_2), there is a stable, tumor-free equilibrium point. In this case, the immune system is effective in fighting the tumor and in principle no treatment would be required. However, with coefficients in Table 2.1, $a_1 d_2 = 10^{-5}$ and $b_2 c_1 = 10^{-4}$: this is case 2 with P_1 unstable and P_2 stable. Quantitatively, we have $\lambda_1 = -0.005$, $\lambda_2 = -0.005$, $\lambda_3^{(1)} = -\lambda_3^{(2)} = 0.018$, $\lambda_4 = -0.010$, $\lambda_5 = -0.002$.

The two equilibria of the tumor-immune model (2.1) are characterized by the fact that there are neither dendritic cells (D), nor IL-2 (I) when the system is at rest. The CD4 (H) and CD8 (C) T-cell are in a steady state which is equal to the ratio between birth and death rate, a_0/c_0 and a_1/c_1, respectively. The tumor concentration

at the two equilibria makes a big difference. The first point has no tumor and it is unstable. The second, stable point has a tumor concentration close to the carrying capacity of the tumor itself (0.9 in this case). These features are similar to those observed in [11] with the third-order model. It is worth mentioning that the stability properties depend on the model coefficients, which have been tuned to reproduce the same qualitative behavior in [11] (see [16]). It could be that there exist a proper combination of a_1, c_1, b_2, c_2 such that the features found above are reversed (i.e., P_1 stable, P_2 unstable), though there is an order of magnitude between $a_1 d_2 = 10^{-5}$ and $b_2 c_1 = 10^{-4}$. In summary, with system (2.1) and coefficients in Table 2.1, there is no complete clearance of the tumor in the non-treatment case ($u = 0$). For this situation, in this paper we show that it is possible to enhance the immune response with immunotherapy under an optimal control perspective.

4. Optimal control problem. The control term u is now introduced and the optimal control problem is discussed in this section. The general optimal control problem is formulated in Section 4.1, where the limitations of an indirect approach, relying on the Euler–Lagrange equations, are recalled. In Sections 4.2 and 4.3 the direct transcription procedure is derived to solve both the continuous and discrete control problems, respectively. The idea of our method is to use a direct approach to treat continuous and discrete optimal control problems deemed "particularly challenging" [17]. We show how these two kind of problems can be solved with direct transcription and collocation (continuous control) or direct transcription and multiple shooting (discrete control). The numerical results achieved for both controls are presented in Section 5.

4.1. Statement of the problem. Let $\mathbf{y} = (y_1, y_2, y_3, y_4, y_5)^T = (H, C, M, D, I)^T$ be a generic state, and let dynamics (2.1) be re-written in the form

$$\dot{\mathbf{y}} = \mathbf{f}(\mathbf{y}(t), u(t)), \tag{4.1}$$

where $\mathbf{f}$ is the right-hand side vector field in (2.1), $u(t)$ is the drug injection as it appears in (2.1), and t is the time. In order to define an optimal control problem, a functional cost has to be identified. As first goal, one attempts to minimize the final tumor concentration, and therefore the objective function could be defined as

$$J = y_3(t_f), \tag{4.2}$$

where t_f is the final time. Although having $y_3(t_f) \simeq 0$ would be desirable, the objective function (4.2) poses no limits on the control in the arc $[t_0, t_f]$, being t_0 the initial time. The maximum amount of drug administerd has to be limited. Without any assumption on the control as in [11], the tumor cells are cleared, but the immune system grows without any bounds. These aspect can cause side effects that may compromise the outcome of the therapy. The performance index adopted in the analysis below takes into account these side effects through the introduction of a control penalty that prevents the indiscriminate immune system growth and therefore limits the toxicity of the treatment. The objective function considered is

$$J = \rho\, y_3(t_f) + \frac{1}{2}\int_{t_0}^{t_f} u^2 \mathrm{d}t \tag{4.3}$$

where ρ is a weighting factor used to balance the two contributions. Objective function (4.3) attempts to find a compromise between final tumor concentration and the

amount of drug injected along the treatment. As for the initial conditions, we assume that the initial state is fully known for a given patient; i.e.,

$$\mathbf{y}(t_0) = \mathbf{y}_0 \tag{4.4}$$

where $\mathbf{y}_0$ is the given initial condition.

Dynamics (4.1), together with objective function (4.3) and initial condition (4.4) define the optimal control problem. This problem is usually tackled by solving the Euler–Lagrange equations

$$\dot{\mathbf{y}} = \frac{\partial H}{\partial \boldsymbol{\lambda}}, \qquad \dot{\boldsymbol{\lambda}} = -\frac{\partial H}{\partial \mathbf{y}}, \qquad 0 = \frac{\partial H}{\partial u}, \tag{4.5}$$

where $H(\mathbf{y}, \boldsymbol{\lambda}, u, t) = 1/2\, u^2 + \boldsymbol{\lambda}^T \mathbf{f}(\mathbf{y}, u)$ is the Hamiltonian of the problem, and $\boldsymbol{\lambda} = (\lambda_1, \lambda_2, \lambda_3, \lambda_4, \lambda_5)^T$ is the 5-dimensional vector of costates or Lagrange multipliers [23]. System (4.5) is supplemented by the boundary conditions

$$\mathbf{y}(t_0) = \mathbf{y}_0, \quad \boldsymbol{\lambda}(t_f) = (0, 0, \rho, 0, 0)^T. \tag{4.6}$$

Equations (4.5)–(4.6) define a differential-algebraic parametric two-point boundary value problem. However, for the case at hand, the last of Eqs. (4.5) reads

$$u + \lambda_4 = 0 \tag{4.7}$$

which in turn yields $u = -\lambda_4$. This condition can be substituted into the first two Eqs. (4.5) yielding a classic, purely differential two-point boundary value problem. Once this problem is solved, the functions $\mathbf{x}(t)$, $\boldsymbol{\lambda}(t)$, $t \in [t_0, t_f]$, are known and the nominal, optimal protocol therapy $u(t)$ is defined through (4.7). Nevertheless, the numerical solution of this two-point boundary value problem requires guessing either the costates at initial time (for shooting method) or their value along the therapy (for collocation method). In any case, their lacking of biological meaning, together with the highly nonlinear dynamics characterizing system (4.5), makes the solution of problem (4.5)–(4.7) quite difficult [17]. For this reason, we transform this differential problem into a nonlinear programming (NLP) problem using the approach described in [24]. This method allows handling the two different control strategies, which are described in the following subsections.

4.2. Continuos control. From the clinical point of view, continuos control in the therapy practice consists in the drug administration assuming a defined flow rate. To this aim, syringe pump provides an affordable solution to sophisticated dispensing and flow control applications. To solve the continuous control case, the problem (4.3)–(4.6) is transformed into a NLP problem by using direct transcription and collocation, following the nomenclature in [21, 24]. The time domain $[t_0, t_f]$ is split into $N - 1$ steps using N mesh points; i.e.,

$$t_j = t_0 + (j-1)\frac{t_f - t_0}{N-1}, \qquad j = 1, \ldots, N. \tag{4.8}$$

Both the states and the control are discretized over the uniform grid (4.8); i.e., $\mathbf{y}_j = \mathbf{y}(t_j)$ and $u_j = u(t_j)$, respectively. The $6N + 1$ NLP variable vector is defined as

$$\mathbf{x} = (\mathbf{y}_1, u_1, \mathbf{y}_2, u_2, \ldots, \mathbf{y}_N, u_N, t_N)^T, \tag{4.9}$$

where the final time t_N is included as optimization variable to search for optimal therapy duration. Dynamics (4.1) are integrated by defining $5(N-1)$ defects

$$\boldsymbol{\zeta}_k = \mathbf{y}_{k+1} - \mathbf{y}_k - \frac{h}{6}(\mathbf{f}_k + 4\hat{\mathbf{f}} + \mathbf{f}_{k+1}), \qquad k = 1, \ldots, N-1 \tag{4.10}$$

where the Hermite–Simpson rule is used; $\mathbf{f}_k = \mathbf{f}(\mathbf{y}_k, u_k)$, $h = t_{k+1} - t_k$. The quantity $\hat{\mathbf{f}}$ is defined as

$$\hat{\mathbf{f}} = \mathbf{f}(\hat{\mathbf{y}}, t_k + h/2), \qquad \hat{\mathbf{y}} = \frac{\mathbf{y}_{k+1} + \mathbf{y}_k}{2} + \frac{h}{8}(\mathbf{f}_k - \mathbf{f}_{k+1}) \tag{4.11}$$

The initial condition (4.4) is transcribed as

$$\Phi_0 = \mathbf{y}_1 - \mathbf{y}_0. \tag{4.12}$$

Using Eqs. (4.10) and (4.12), the $5N$-dimensional vector of nonlinear equality constrains reads

$$\mathbf{c}(\mathbf{x}) = \left\{\Phi_0, \boldsymbol{\zeta}_1, \boldsymbol{\zeta}_2, \ldots, \boldsymbol{\zeta}_{N-1}\right\}^T. \tag{4.13}$$

The last step consists in defining the functional cost (4.3) using the NLP formalism and the variable vector (4.9). This is done through a trapezoidal integration scheme:

$$J(\mathbf{x}) = \rho\, x_{6N-3} + \frac{1}{2}\sum_{i=1}^{N-1}(x_{6(i+1)}^2 + x_{6(i)}^2)(t_{i+1} - t_i). \tag{4.14}$$

The NLP problem can be stated as

$$\min_{\mathbf{x}} J(\mathbf{x}) \quad \text{subject to} \quad \mathbf{c}(\mathbf{x}) = 0. \tag{4.15}$$

The advantage of having formalized the optimal control problem as a standard NLP problem (4.15) is that the latter can be solved with standard optimization software, so avoiding the explicit derivation of necessary conditions of optimality. (In this work, we have used the routine `fmincon` implemented in Matlab [25].) With the problem stated as in (4.15), the optimization has not to deal with Lagrange multipliers (at least at high level implementation), whose lack of meaning prevents the formulation of appropriate guesses. When (4.15) is solved, the optimal drug administration policy u_j is known at discrete times t_j. The function $u(t)$, $t \in [t_0, t_f]$ can be reconstructed, for instance, through spline interpolation. Thus, although dynamics are discretized with direct transcription and collocation, this method delivers continuous control laws. This is not the case of the control strategy considered next.

4.3. Discrete control. Discrete control is introduced to fit the need of actual protocol procedures. In medical practice, indeed, administrations are made for short periods of time, separated by intervals of drug holidays. The time scale of administration (seconds or minutes) is orders of magnitude shorter than the typical time scale of the tumor-immune interaction (hours). For this reason, considering the administration as impulsive is a good approximation [17]. Such approximation can no longer be modeled with (4.3)–(4.6) since impulsive control produces discrete changes in the system dynamics. Thus, the problem needs to be re-formulated to accommodate for impulsive input. Discrete control is treated with direct transcription and multiple shooting strategy [21]. With this method, the time domain $[t_0, t_f]$ is divided

into m nonuniformly spaced segments $[t_0, t_1, \ldots, t_m]$, and m impulsive controls u_j are introduced at t_j, $j = 1, \ldots, m$. The m drug holiday periods are $\Delta t_j = t_j - t_{j-1}$, $j = 1, \ldots, m$.

The problem is stated as follows. Let $\phi(\mathbf{y}_0, t_0, t)$ be the flow of (4.1) at time t starting from t_0 with initial condition $\mathbf{y}_0$. The integration within $[t_0, t_1]$ yields the state immediately before the control; i.e., $\mathbf{y}_1^- = \phi(\mathbf{y}_0, t_0, t_1)$. The control u_1 is then instantaneously applied at t_1. The structure of (2.1) suggests that an impulsive control would modify the value of the fourth component only. Thus, the state immediately after the first injection is $\mathbf{y}_1^+ = \mathbf{y}_1^- + (0, 0, 0, 1, 0)^T u_1$. This permits us to integrate the dynamics (4.1) within $[t_1, t_2]$. At time t_2, the second injection is introduced through $\mathbf{y}_2^+ = \mathbf{y}_2^- + (0, 0, 0, 1, 0)^T u_2$, with $\mathbf{y}_2^- = \phi(\mathbf{y}_1^+, t_1, t_2)$. In general, the following procedure is repeated

$$\mathbf{y}_j^- = \phi(\mathbf{y}_{j-1}^+, t_{j-1}, t_j), \quad \mathbf{y}_j^+ = \mathbf{y}_j^- + (0, 0, 0, 1, 0)^T u_j, \quad j = 1, \ldots, m. \tag{4.16}$$

In analogy with (4.14), the objective function attempts to minimize both the final tumor mass $y_{3,m}$ and the amount of administered drug through

$$J = \rho\, y_{3,m} + \sum_{j=1}^{m} u_j. \tag{4.17}$$

where ρ is again a weighing coefficient.

Problem (4.15)–(4.16) is transformed into a NLP problem by introducing the variable

$$\mathbf{x} = (u_1, u_2, \ldots, u_m, \Delta t_1, \Delta t_2, \ldots, \Delta t_m). \tag{4.18}$$

It is easy to rewrite both the procedure (4.16) and the performance index (4.17) in terms of $\mathbf{x}$. The parametric optimization problem is then

$$\min_{\mathbf{x}_{lb} \le \mathbf{x} \le \mathbf{x}_{ub}} J(\mathbf{x}) \quad \text{subject to} \quad \mathbf{g}(\mathbf{x}) \le 0 \tag{4.19}$$

where the vector of inequality constraints, $\mathbf{g}(\mathbf{x}) = \mathbf{y}(\mathbf{x})_j^+ - \mathbf{1}$, $j = 1, \ldots, m$, prevents the indefinite growth of the immune system cells as a side effect of a strong therapy. The lower and upper bounds are

$$\begin{aligned} \mathbf{x}_{lb} &= (u_1^{\min}, \ldots, u_m^{\min}, \Delta t_1^{\min}, \ldots, \Delta t_m^{\min})^T, \\ \mathbf{x}_{ub} &= (u_1^{\max}, \ldots, u_m^{\max}, \Delta t_1^{\max}, \ldots, \Delta t_m^{\max})^T, \end{aligned} \tag{4.20}$$

with $u_j^{\min}$, $u_j^{\max}$ is the minimum, maximum amount of administrable drug at t_j, respectively; $\Delta t_j^{\min}$, $\Delta t_j^{\max}$ is the minimum, maximum j-th drug holiday, respectively. The optimization (4.19) finds *when* and *how much* drug has to be administered.

4.3.1. Direct search of initial guess solutions. The effectiveness of gradient search, iterative methods (used to solve problem (4.19)) in converging to an optimal solution depends on the initial guess provided. In order to provide good initial guesses to problem (4.19), a Genetic Algorithm (GA) optimization is run [26]. This step is useful to explore the entire domain of feasible solutions, and to find preliminary values of both drug administrations (u_j) and drug holidays (Δt_j). The GA step exploits the knowledge of the search space, which is defined by (4.20). (In this work we have used the Matlab built-in genetic algorithm `ga` [27].)

The GA step minimizes (4.17) with a penalty to account for the inequality constrains. The solution so derived is treated as initial guess to solve the local optimization problem (4.19). Note that the solution found by the GA would not likely respect the inequality constraints in (4.19). These are explicitly imposed in the subsequent NLP step. This combined approach (GA + NLP) is usually referred to as "hybrid optimization".

5. Optimal Protocol Examples. Both continuous and discrete optimal protocol therapies are shown. The initial condition used for both cases is reported in Table 5.1. This initial condition has cells concentration having the same value except for tumor concentration that is six times higher. In this case, tumor cell concentrations is above 50% of its carrying capacity, and the other cell concentrations show values averaged among those presented in literature [13]. The value of ρ used in both (4.14) and (4.17) is 1.75.

Cell	Helper (y_1)	Cytotoxic (y_2)	Tumor (y_3)	Dendritic (y_4)	IL2 (y_5)
Concentration	0.1	0.1	0.6	0.1	0.1

TABLE 5.1
Initial patient condition considered in the optimization problems.

5.1. Optimal continuous protocol. The NLP problem (4.15) is solved using $N = 150$ mesh points, which means having 901 NLP variables according to (4.9). In order to have algorithm convergence, the optimization starts with a coarse mesh made up by 25 points with $\mathbf{x}_i = (0.5, 0.5, 0.5, 0.5, 0.5)$, $i = 1, ..., 25$. The solution obtained is then interpolated over a mesh implementing 25 more points. With five refinement loops, a mesh of 150 points is achieved. The final solution is obtained after 131 iterations with a relative tolerance on the functional cost at two consecutive iterations set to 10^{-6}. The complete analysis (solution of 6 NLP problems) takes 24500 s on an Intel Centrino Dual Core 1.66MHz, 1 Gb Ram laptop. (These computer features apply also to all following examples).

Direct transcription approximates the problem with the Hermite–Simpson integration scheme. The resulting solution is verified by numerical integration adopting a 7th/8th order Runge–Kutta integration scheme with absolute and relative tolerances set to 10^{-8}. The forward integration is carried out taking the optimal first grid point y_1 as initial condition, and with a cubic spline of the controls u_j. This higher order method is useful to evaluate the accuracy of the solutions found, here obtained with a low-order method. The following condition is evaluated

$$\|\mathbf{y}(t_f) - \mathbf{y}_N\| \leq \epsilon \tag{5.1}$$

where $\mathbf{y}(t_f)$ is obtained through the Runge–Kutta integration, while $\mathbf{y}_N$ is obtained with the Hermite–Simpson integration. The tolerance ϵ is set to 10^{-4}. The grid is refined if (5.1) is not respected; otherwise, the optimization terminates.

Figure 5.1 shows an optimal solution with continuous control. The optimized control consists in a diffused continuous administration during the entire therapy (Fig. 5.1(b)). When the concentration of dendritic cells is increasing (maximum value reached at day 130), the dosage of the injection decreases in order to satisfy the constraint on the carrying capacity. At day 134 the control stops decreasing and increases again, until day 291 where the tumor concentration reverts the sign of the

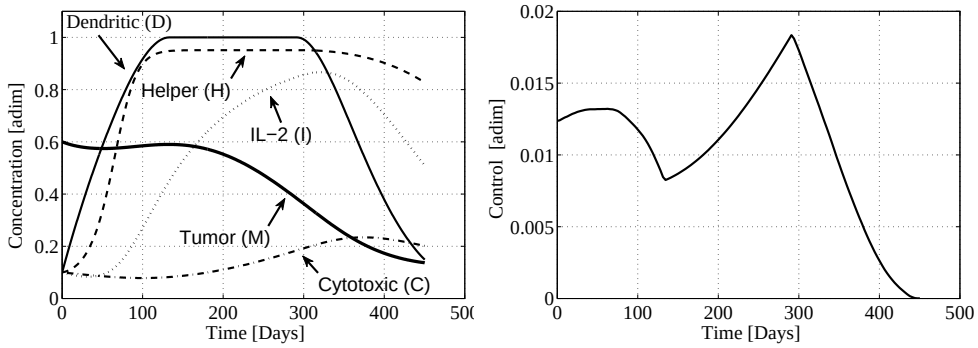

(a) State variables (b) Control

FIG. 5.1. *Optimal therapy with continuous control.*

second derivative. At day 370, the concentration level of IL-2 reaches its maximum. After this point the control decreases and goes to zero. The tumor dynamics varies accordingly with a decreasing trend. The therapy lasts 450 days and the tumor concentration drops from 0.6 to 0.137 (77% reduction).

5.2. Optimal discrete protocols. The discrete optimization problem has been solved with $m = 18$ injections. The lower and upper bounds (4.20) are: $u_i^{\min} = 0$, $\Delta t_i^{\min} = 10$ days, $u_i^{\max} = 1$, $\Delta t_i^{\max} = 100$ days. The hybrid algorithm combines global and local search through GA and NLP. The population size at each generation is made up by 100 individuals. Through numerical experiments, this number has been deemed adequate to sufficiently explore the search space. The maximum number of generation is fixed at 1000. The algorithm converges when the difference in the functional cost of two consecutive generations is less then 10^{-6}. The GA determines an intermediate solution after 275 generations. This solution has a final tumor concentration of 0.067, though it is useless as it does not respect the inequality constrains. Nevertheless, this is the initial point for the gradient-based algorithm used to solve the NLP problem. The latter converges to the optimal solution in 35 iterations (relative tolerance set to 10^{-6}). The total computational time is 759 s. Using this approach based on the multiple shooting technique a verification of the solution is not required because within each interval the system is integrated with a 7th/8th order Runge–Kutta.

Figure 5.2 shows an optimized result obtained with the hybrid approach. One of the relevant features of the results consists in the amount and frequency of the injections (Fig. 5.2(b)) that we discuss next. Starting from day 0, the neoplasia decreases for few days, after which it tends to grow with no control; meanwhile the value of dendritic cells decreases to accommodate a high injection dose (the level of dendritic cells after the injection must be less than or equal to 1). The control prevents the tumor growth with a first injection (administered at about day 200), which is the one with the highest dosage. This first stage with low frequency, high dosage lasts until day 300, when the tumor stops increasing. During this period the control counteracts tumor cells growing, and at the same time allows increasing the concentration of Interleukin-2. This is done by keeping both Dendritic cells and Helper cells close to their carrying capacity. Once at this stage, the role of IL-2 is to create an environment that stimulates the growth of the immune system cells.

When the trend of both Tumor and Cytotoxic cells is reversed (the former de-

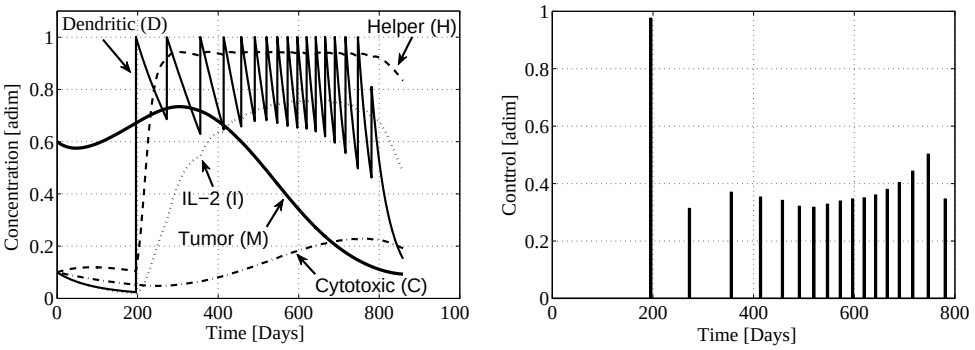

(a) State variables (b) Control

FIG. 5.2. *Optimal therapy with discrete control.*

creases, the latter increases), the optimal control strategy enters a new phase. Starting from the fourth injection (at day 410) the frequency increases while the drug dosage decreases. This keeps the Helper cells concentration close to the carrying capacity for a long time, and it is at this stage that the most enforcement efforts on the tumor reduction are obtained. In a period of time similar to that of the first phase, the tumor mass is reduced by over 60%, thanks to the growth of cytotoxic cells population. The optimal protocol presents then a final stage in which the frequency is low again (last two injections). This stage, that we can define conservation, serves to maintain the concentration of tumor cells at the levels achieved in the previous period. The final tumor concentration is reduced to 0.093 from 0.6 (84% reduction); the therapy lasts less than 600 days (the first injection is at day 200).

The structure of the solution therapy is influenced by the number of injections, m, and this parameter is the one that mostly influences the performances of the method. This value cannot be added to the optimization variables, as the NLP formulated in (4.19) can accommodate continuous variables only (and facing mixed integer-continuous optimizations is out of the scope of the paper). However, a parametric analysis has been performed in order to evaluate the optimal solutions' features for variable m. The results are reported in Table 5.2. The cases $m = 5, 10, 15, 10, 25$ have been considered, and the associated five optimal control problems have been solved. For each solution we have kept track of the final tumor concentration ($M(t_f)$), the maximum value of tumor along the therapy ($\max M$), the final time (t_f), and the total amount of drug administered ($\sum_{j=1}^{m} u_j$). As expected, there is no direct proportionality between the number of injections and the final tumor concentration. The minimum final concentration is found for $m = 15$ ($M(t_f) = 0.1091$). On the contrary,

m	$M(t_f)$	$\max M$	t_f	$\sum_{j=1}^{m} u_j$
5	0.3846	0.6156	499.45	3.1211
10	0.1980	0.6221	681.96	5.3004
15	0.1091	0.6238	753.08	6.9670
20	0.1132	0.8576	1268.5	6.8784
25	0.1211	0.8973	1871.3	6.6202

TABLE 5.2
Features of the therapy for variable number of injections.

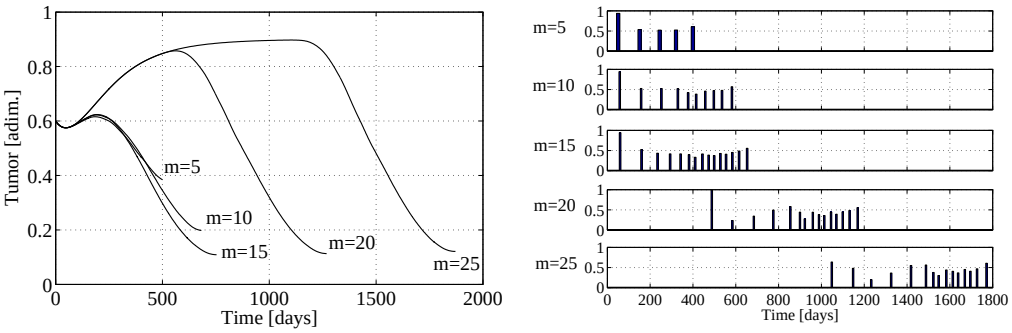

(a) Tumor concentration. (b) Optimal protocols.

FIG. 5.3. *Tumor cells concentration and optimal protocols for variable number of injections.*

there is evidence that the maximum value of tumor along the therapy increases for increasing m. For $m = 5, 10, 15$ this maximum stays about the initial tumor value (0.6); for $m = 20, 25$, the maximum increases up to reach the value 0.8973 for $m = 25$. The final time increases with m too, thought this value is not indicative of the therapy duration. The total amount of drug administered is maximum for $m = 15$ (6.9670). This analysis indicates that the best number of injections is defined across $m = 15$. For such a value, it is possible to reach a final tumor concentration which is less than 80% of the initial concentration, while keeping at same time the global maximum to values about the initial condition. For this reason we have chosen $m = 18$ in the analysis above, where an 84% tumor reduction has been achieved. The results of this parametric analysis are also shown in Fig. 5.3, where the tumor trend and the optimal protocol are reported for variable m. For $m = 20, 25$, although a high number of injections is required, the algorithm drives the amount of some of them to zero, so producing long free-treatment periods according to the structure of the optimization variable in (4.18). This is the best theoretical solution that minimizes (4.17), although it is not likely the best clinical solution.

6. Monte Carlo Analysis. Both protocols (continuous and discrete) have been evaluated for a given, fixed initial condition. In practice, the patient conditions are known with a non-negligible error. Due to the nonlinearities characterizing system (2.1), the dynamics in off-nominal conditions is not easily predictable. Thus, it is necessary to evaluate the protocol effectiveness when the optimal therapy (obtained with nominal initial conditions) is considered in conjunction with off-nominal initial conditions. The robustness of both continuous and discrete controls, as well as the sensitivity of the model to small changes in initial conditions are evaluated through a Monte Carlo analysis. This analysis keeps track of the initial and final value of the tumor mass.

Let $\mathbf{y}_0 = (H_0, C_0, M_0, D_0, I_0)^T$ be the vector of nominal initial conditions (Table 5.1), and let $\mathbf{y}_0^i = (H_0^i, C_0^i, M_0^i, D_0^i, I_0^i)^T$ be the i-th off-nominal initial condition. This is given by

$$y_{0,k}^i = (1 + \delta_k^i)\ y_{0,k}, \qquad k = 1, \ldots, 5, \qquad i = 1, \ldots, n_s, \tag{6.1}$$

with $\delta_k^i \in [-0.1,\ 0.1]$. (The quantity n_s in (6.1) indicates the total number of samples.) Equation (6.1) states that a 10% uncertainty is assumed in the initial conditions. The

Dynamics	μ_0	σ_0	μ_f	σ_f
Natural	0.6011	0.0566	0.8852	0.0095
Continuous control	0.5999	0.0584	0.1289	0.0456
Discrete control	0.6024	0.0573	0.0914	0.0034

TABLE 6.1
Statistics of the Monte Carlo analysis.

i-th off-nominal initial condition is integrated under system (2.1) through

$$\mathbf{y}_f^i = \phi(\mathbf{y}_0^i, t_0, t_f, \hat{u}) \tag{6.2}$$

where $\hat{u}$ is either null (natural dynamics) or equal to the continuous, discrete optimal controls associated to $\mathbf{y}_0$. The i-th final state is labelled $\mathbf{y}_f^i = (H_f^i, C_f^i, M_f^i, D_f^i, I_f^i)^T$. The effectiveness of the administration protocol is assessed by statistics on both M_0^i and M_f^i. In practice, we compute the average μ and standard deviation σ of M_0^i and M_f^i samples in either natural or controlled dynamics.

A set of 10^3 off-nominal initial conditions $\mathbf{y}_0^i$ is constructed by random generation of δ_k^i. These samples are integrated with (6.2) and the initial, final average $\mu_{0,f}$ and standard deviation $\sigma_{0,f}$ are computed. These are reported in Table 6.1. We recall that the nominal initial values of tumor mass is $M_0 = 0.60$, whereas the nominal final values are $Mf = 0.137$ (for continuous control) and $M_f = 0.093$ (for discrete control). It can be seen that in the case of natural dynamics the final tumor mass grows up to high values whose average is 0.8852; the standard deviation decreases instead from about 5% to less than 1% at final time. The controlled case shows low values of final tumor mass with average 0.1289 (continuous control) and 0.0914 (discrete control); the final standard deviation is 4.5% in the continuous case and 0.3% in the discrete one. From these features, there is evidence that the optimal administration protocol derived with nominal conditions can be effectively used even in off-nominal cases, provided that the initial mismatch (between nominal and non-nominal conditions) is acceptable. Figure 6.1 shows more clearly the convergence of the system to the nominal solution. The trajectory of tumor mass is shown in both nominal and extreme off-nominal conditions (min and max M_0^i and M_f^i) in both continuous and discrete controls. It can be seen that the treatment is robust with respect to variation of initial conditions as the final goal of reducing the tumor mass is achieved. The smaller final standard deviation of the discrete control can be appreciated.

7. Conclusion. The problem of cancer immunotherapy is studied in this paper with mathematical means. A fifth-order model has been assumed to describe the dynamics of the tumor-immune interaction. This model is specialized for autologous dendritic cell transfection therapy, and therefore the input to the model is represented by dendritic cells. Besides dendritic cells, the other system states are helper CD4 T-cell, cytotoxic CD8 T-cell, tumor cells, and Interleukin-2. Analyzing the system at rest shows that there are two equilibrium points characterized by null and high values of tumor mass, the former being unstable and the latter stable with the model parameters assumed. Under these assumptions, the appearance of tumor cells in a tumor-free state triggers the growth of the tumor itself. A treatment is required to fight the tumor. Among all possible treatments, we choose a therapy protocol based on dendritic cell transfection. This therapy is formalized as an optimal control problem.

The optimal drug administration control problem has been formulated and solved

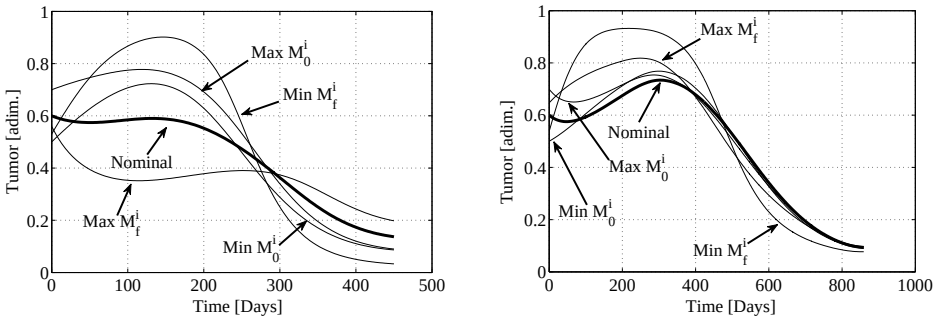

(a) Continuos control. (b) Discrete control.

FIG. 6.1. *Tumor cells concentration trend associated to different initial conditions integrated under the continuous control (Fig. 5.1(b)) and the discrete control (Fig. 5.2(b)).*

with two different control strategies. The continuous control case has been solved with direct transcription and collocation. This approach shows a reduction of the tumor mass, though a continuous control involves hard limitations on clinical applications as the injection flow rate needs to be controlled for hundreds of days. A way to consider real medical practice consists in formulating the protocol therapy as made up by discrete injections. From a mathematical point of view these can be modeled as instantaneous, impulsive controls. Drug holiday, needed to bring down the therapy toxicity, are explicitly taken into account with this approach. Discrete control has been solved via direct transcription and multiple shooting technique, with a first guess solution determined with a genetic algorithm. Achieved results show that not only this strategy is feasible at clinical level, but also that the tumor concentration is reduced to about 16% of its initial value (22% in case of continuous control).

The robustness of discrete-control therapy has been assessed with a Monte Carlo analysis where the optimal protocol is applied to off-nominal initial conditions. Statistical results indicates that even in off-nominal cases the tumor mass is effectively reduced, so showing the validity of the optimal therapy protocol in real cases where the patient conditions are not exactly known.

In the two cases presented, the discrete control outperforms the continuous control in terms of final tumor value. Discrete control involves less optimization variables than the continuous control (36 and 901 variables, respectively), and it is much more efficient from a computational point of view (about 96% less computational time). Moreover, the discrete control behaves better in off-nominal conditions by showing a smaller final standard deviations than the continuous control. These results, together with the feature of being better applicable in real medical practice, let us lean toward the discrete control strategy.

The two optimal control strategies are general and can be fully automated once the initial patient conditions are know with sufficient confidence level. The solution strategy based on direct transcription and collocation (continuous case) or multiple shooting (discrete case) avoids dealing with both the Euler–Lagrange equations and their associated two-point boundary value problems; this approach can be though as an alternative to those described in literature [12, 13, 16, 17].

It is worth mentioning that both qualitative and quantitative results depend on the model parameters and initial condition considered, and therefore any generalization of these results to clinical conclusions would at this stage be completely haz-

ardous. Despite this, the results show that an approach through the theory of optimal control is both efficient and effective in order to solve problems of cancer immunotherapy.

Acknowledgements. The authors are grateful to Prof. G. Parmiani and Dr. T. Di Tomaso of Università Vita–Salute San Raffaele (Milan, Italy) for their professional and useful feedback provided. The authors would like to thank Dr. F. Castiglione of Istituto per le Applicazioni del Calcolo, Consiglio Nazionale delle Ricerche (Rome, Italy) for useful discussions on the dynamical model and optimal control results. The authors express their gratitude to the anonymous reviewers whose comments and constructive suggestions have improved the overall quality of the paper.

REFERENCES

[1] A. Jemal, R. Siegel, E. Ward, Y. Hao, J. Xu, and M. J. Thun, Cancer Statistics CA Cancer Journal for Clinicians, 59 (2009), pp. 225–249.
[2] S. A. Rosemberg, J. Yang, S. Topalian, D. Schwartzentruber, J. Weber, D. Parkinson, C. Seipp, J. Einhorn, D. White Treatment of 283 Consecutive Patients with Metastatic Melanoma or Renal Cell Cancer using High Dose Bolus Interleukin 2, Journal of the American Medical Association, 271 (1994), pp. 907–913.
[3] P. J. Bergman, Cancer Immunotherapy, Topics in Companion Animal Medicine, 24 (2009), pp. 130–136.
[4] P. J. Delves, S. J. Martin, D. R. Burton, and I. M. Roitt, Essential Immunology, Blackwell Publishing, Malden, MA, 2006.
[5] M. McClellan, J. Yang, H. Pass, W. Linehan, and S. Rosemberg, Cytoreductive Surgery before High Dose Interleukin 2 Based Therapy in Patients with Metastatic Renal Cell Carcinoma, Journal of Urology, 158 (1997), pp. 1675–1678.
[6] S. A. Rosemberg and M. E. Dudley, Adoptive Cell Therapy for the Treatment of Patient with Metastatic Melanoma, Current Opinion in Immunology, 21 (2009), pp. 233–240.
[7] L. Preziosi, Cancer Modeling and Simulation, Chapman & Hall/CRC, Boca Raton, FL, 2003.
[8] L. Preziosi, Modelling Tumour Growth and Progression, In A. Buikis, R. Ciegis & A.D. Fitt, (Eds.), Progress in Industrial Mathematics at ECMI 2002, Springer, pp. 53– 66,2004.
[9] G. Caravagna, A. D'Onofrio, P. Milazzo, and R. Barbuti, Tumor Suppression by Immune System through Stochastic Oscillations, Journal of Theoretical Biology, 265 (2010), pp. 336–345.
[10] F. Pappalardo, M. Pennisi, F. Castiglione, and S. Motta, Vaccine Protocol Optimizations: In Silico Experiences, Biotechnology Advances, 28 (2010), pp. 82–93.
[11] D. Kirschner and J. C. Panetta, Modeling Immunotherapy of the Tumor-Immune interaction, Journal of Mathematical Biology, 37 (1998), pp. 235–252.
[12] T. Burden, J. Ernstberger, and K. R. Fister, Optimal Control Applied to Immunotherapy, Discrete and Controlled Dynamical Systems, 4 (2004), pp. 135–146.
[13] A. Cappuccio, F. Castiglione, and B. Piccoli, Determination of the Optimal Therapeutic Protocols in Cancer Immunotherapy, Mathematical Bioscience, 209 (2007), pp. 1–13.
[14] D. Kirschner and A. Tsygvintsev, On the Global Dynamics of a Model for Tumor Immunotherapy, Journal of Mathematical Biosciences and Engineering, 6 (2009), pp. 573–583.
[15] A. Cappuccio, M. Elishmereni, and Z. Agur, Cancer Immunotherapy by Interleukin-21: Potential Treatment Strategies Evaluated in a Mathematical Model, Cancer Research, 66 (2006), pp. 7293–7300.
[16] F. Castiglione and B. Piccoli, Optimal Control in a Model of Dendritic Cell Transfection Cancer Immunotherapy, Bulletin of Mathematical Biology, 68 (2006), pp. 255–274.
[17] F. Castiglione and B. Piccoli, Cancer Immunotherapy, Mathematical Modeling and Optimal Control, Journal of Theoretical Biology, 247 (2007), pp. 723–732.
[18] M. Pennisi, C. Bianca, F. Pappalardo, and S. Motta, Modeling Artificial Immunity against Mammary Cancer, Proceedings of the 10^{th} International Conference on Computational and Mathematical Methods in Science and Engineering, 2010, pp. 753–756.
[19] O. G. Isaeva and V. A. Osipov, Different Strategies for Cancer Treatment: Mathematical Modeling, Computational and Mathematical Methods in Medicine, 10 (2009), pp. 253–272.
[20] L. G. De Pillis and A. Radunskaya, The Dynamics of an Optimally Controlled Tumor Model: A Case Study, Mathematical and Computer Modeling, 11 (2003), pp. 1221–1244.

[21] J. T. Betts, Survey of numerical Methods for Trajectory Optimization, Journal of Guidance, Control, and Dynamics, 21 (1998), pp. 193–207.
[22] F. Kozusko and Z. Bajzer, Combining Gompertzian Growth and Cell Population Dynamics, Mathematical Bioscience, 185 (2003), pp. 153–167.
[23] A. Bryson and Y. Ho, Applied Optimal Control, Hemisphere, Washington, 1975.
[24] J. T. Betts, Practical Methods for Optimal Control using Nonlinear Programming, SIAM, Philadelphia, 2000.
[25] Optimization Toolbox Users Guide, The MathWorks, Inc., 2003.
[26] D. E. Goldberg, Genetic Algorithms in Search Optimization and Machine Learning, Addison Wesley, 1989.
[27] Genetic Algorithm and Direct Search Toolbox Users Guide, The MathWorks, Inc., 2009.